

NONLINEAR ROCKING MOTIONS. I: CHAOS UNDER NOISY PERIODIC EXCITATIONS

By H. Lin¹ and S. C. S. Yim,² Member, ASCE

ABSTRACT: The effects of low-intensity random perturbations on the stability of chaotic response of rocking objects under otherwise periodic excitations are examined analytically and via simulations. A stochastic Melnikov process is developed to identify a lower bound for the domain of possible chaos. An average phase-flux rate is computed to demonstrate noise effects on transitions from chaos to overturning. A mean Poincaré mapping technique is employed to reconstruct embedded chaotic attractors under random noise on Poincaré sections. Extensive simulations are employed to examine chaotic behaviors from an ensemble perspective. Analysis predicts that the presence of random perturbations enlarges the possible chaotic domain and bridges the domains of attraction of coexisting attractors. Numerical results indicate that overturning attractors are of the greatest strength among coexisting ones; and, because of the weak stability of chaotic attractors, the presence of random noise will eventually lead chaotic rocking responses to overturning. Existence of embedded strange attractors (reconstructed using mean Poincaré maps) indicates that rocking objects may experience transient chaos prior to overturn.

INTRODUCTION

An in-depth understanding of the rocking behavior of rigid block-like structures is essential to mechanical and civil engineers in design and maintenance of a variety of freestanding structures, such as petroleum storage tanks, water towers, nuclear reactors, concrete radiation shields and equipment racks subjected to base excitations including earthquake ground motions, and nearby machine vibrations (Yim and Lin 1991a). It is well known that the rocking response is highly nonlinear and can be very sensitive to small variations in system parameters and excitation details. Probabilistic trends of the response can only be estimated with a large sample size (Aslam et al. 1980; Yim et al. 1980). Classical analytical methods have been developed for piecewise linear approximate models to predict the existence and stability of harmonic and subharmonic responses under periodic excitation (Spanos and Koh 1984; Tso and Wong 1989).

In an experimental study, Wong and Tso (1989) found that there were responses that could not be accounted for by classical analytical methods. These unpredicted responses were further investigated and later identified to be chaotic (Hogan 1989; Yim and Lin 1991b). Hogan (1989) developed a discrete mapping technique to determine the stability regions of harmonic and subharmonic responses, and identified the regions of possible chaotic response. He also quantitatively matched analytical predictions with Wong and Tso's experimental results. Yim and Lin (1991a,b) examined the response behavior of both slender and nonslender rocking objects under periodic excitations and found that, although chaotic time histories have a periodic time dependency, time series consisting of Poincaré points of chaotic responses possess stochastic invariant properties, indicating a strong link between deterministic and stochastic behavior (Yim and Lin 1992).

Chaotic rocking responses have so far been studied under deterministic settings by the authors cited. However, except under artificially strict control (example, "tabletop" experi-

ments), few purely deterministic environment excitations of engineering interest (especially periodic ones) are realized in practice. Environmental uncertainties and disturbances need to be taken into account by incorporating stochastic components in the system excitation model. This two-part study represents a first attempt to expand previous deterministic stability analyses of chaotic rocking responses and relationships between bounded and overturning responses to include stochastic components in the excitations. Specifically, models of freestanding rigid objects, both slender and nonslender, subjected to periodic excitation with random noise perturbations are considered. Part I concentrates on applying analysis techniques to study the relationships between chaotic and overturning responses under the influence of small random perturbations. Part II (Lin and Yim 1996; the companion paper) provides a detailed study of the response behaviors of randomly perturbed rocking objects from a fully probabilistic perspective via the evolution of the probability density governed by the associated Fokker-Planck equation.

Among existing studies, random excitations to the rocking system are often modeled as idealized white noise (Iyengar and Manohar 1991; Dimentberg et al. 1993) because of its mathematical simplicity (Soong and Grigoriu 1992). White noise is a reasonable approximation of the random perturbations when the noise correlation time is much shorter than the system relaxation time (Stratonovich 1967). However, the infinite variance (energy) of idealized white noise infused into the rocking system can not be realized in practice. In this paper, instead of using the ideal white noise model, random perturbation in the excitation is approximated by a Shinozuka band-limited (hence finite variance) noise (Shinozuka 1971). Analytical and numerical techniques are used to demonstrate the characteristics and stability of randomly perturbed rocking responses. Relationships among periodic, chaotic, and overturning responses are analytically demonstrated by a criterion based on generalized Melnikov process as well as the associated average phase flux. By applying the mean Poincaré mapping technique (Kapitaniak 1988), noise-induced randomness in the chaotic responses is averaged out and embedded strange attractors are reconstructed on Poincaré sections. Capabilities and limitations of this mapping technique are discussed.

PHYSICAL MODEL

In this study, a freestanding object is modeled as a rectangular rigid body subjected to horizontal base motion excitation (Fig. 1). Assuming that friction at the interface between the rigid object and the base is sufficiently large so that there is

¹Res. Assoc., Dept of Civ. Engrg., Oregon State Univ., Corvallis, OR 97331.

²Assoc. Prof., Dept of Civ. Engrg., Oregon State Univ., Corvallis, OR. Note. Associate Editor: John Tassoulas. Discussion open until January 1, 1997. Separate discussions should be submitted for the individual papers in this symposium. To extend the closing date one month, a written request must be filed with the ASCE Manager of Journals. The manuscript for this paper was submitted for review and possible publication on August 3, 1995. This paper is part of the *Journal of Engineering Mechanics*, Vol. 122, No. 8, August, 1996. ©ASCE, ISSN 0733-9399/96/0008-0719-0727/\$4.00 + \$.50 per page. Paper No. 11313.

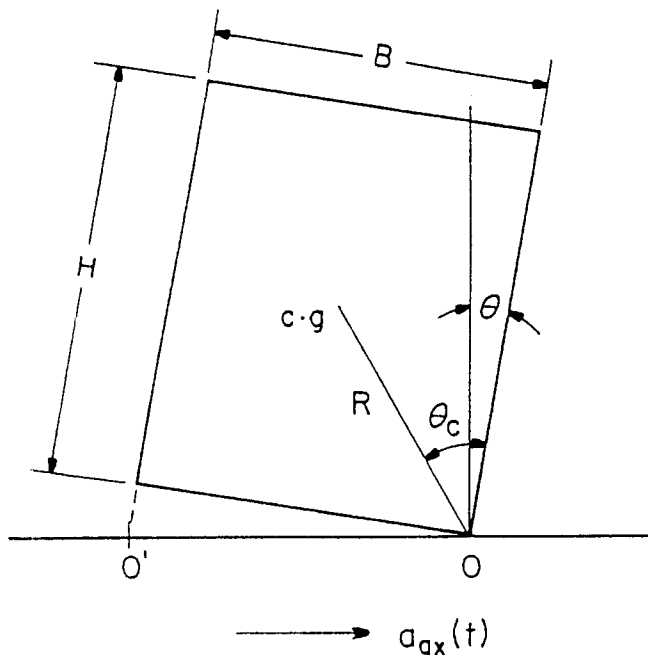


FIG. 1. Idealization of Freestanding Equipment as Rigid Rocking Subjected to Horizontal Excitation

no slipping, depending on the support accelerations, the object may move rigidly with the base or be set into rocking motion (Yim et al. 1980; Yim and Lin 1991a,b). Impact occurs when the angular rotation crosses zero approaching from the positive or negative direction and the base surfaces re-contact. Impact-induced energy loss (or damping) is accounted for by a restitution coefficient, which relates the angular velocities before and after impact (Yim et al. 1980).

The base excitation to the rocking system is assumed to be predominantly periodic. For simplicity, the excitation is approximated by a perturbed sinusoidal forcing. To take into account environmental disturbances, random perturbations in the excitation are approximated by band-limited white noise.

For convenience, a slender (thus piecewise linear) rocking object is considered in this paper, and nondimensionalized governing equations are employed (Yim and Lin 1991a). Taking into account the presence of random perturbations, the governing equations are given by

$$\ddot{\Theta} - \Theta = -A \cos(\Omega\tau + \Psi) + \eta(\tau) - 1, \quad \Theta > 0 \quad (1)$$

and

$$\ddot{\Theta} - \Theta = -A \cos(\Omega\tau + \Psi) + \eta(\tau) + 1, \quad \Theta < 0 \quad (2)$$

with impact transition condition

$$\dot{\Theta}(\tau^+) = e\dot{\Theta}(\tau^-), \quad 0 \leq e \leq 1 \quad (3)$$

where $\Theta = \theta/\theta_c$ is the nondimensionalized angular displacement; and $\tau = \alpha t$ is the nondimensionalized time (with θ = angular displacement, θ_c = critical angle, and t = time). A ($=\alpha a/g$), Ω ($=\omega/\alpha$), and Ψ = nondimensionalized amplitude, frequency, and phase shift of the periodic base excitation, respectively (with a and ω = amplitude and frequency of base excitation). Parameter α is a function of object mass M , mass moment of inertia I_0 , gravitational acceleration g , and radius R (Appendix II); $\tau^-(\tau^+)$ = time just before (after) impact; and e = velocity restitution coefficient. The stochastic process, $\eta(\tau)$, employed here to represent the random perturbations, is given by

$$\eta(\tau) = \sigma \sqrt{\frac{2}{N}} \sum_{n=1}^N \cos(\nu_n \tau + \phi_n) \quad (4)$$

where σ = standard deviation of the noise; and $\{\nu_n, \phi_n; n = 1, 2, \dots, N\}$ are independent random variables defined on a probability space. Frequencies ν_n are nonnegative with a common distribution, and random phase shifts ϕ_n are identically, independently, and uniformly distributed over interval $[0, 2\pi]$ (Shinozuka 1971). It is seen that stochasticity in this model is completely governed by $\eta(\tau)$. In the limit as the noise intensity parameter $\sigma \rightarrow 0$, the excitation approaches purely periodic, and the system behaves in a deterministic fashion. The system response is governed by two linear stochastic differential equations [(1) and (2)] with a local velocity discontinuity at zero displacement [(3)]. This discontinuity causes the rocking response behavior to be highly nonlinear (Yim and Lin 1991a,b).

By introducing state variable vector \mathbf{X}

$$\mathbf{X} = \begin{Bmatrix} x_1 \\ x_2 \end{Bmatrix} = \begin{Bmatrix} \Theta \\ \dot{\Theta} \end{Bmatrix} \quad (5)$$

and including external excitation and energy dissipation as perturbations to (1) and (2), the rocking system can be expressed in vector form and studied in phase space

$$\dot{\mathbf{X}} = \mathbf{f}_{1,2}(\mathbf{X}) + \mathbf{g}(\mathbf{X}, \tau) \quad (6)$$

where

$$\mathbf{f}_1(\mathbf{X}) = \begin{Bmatrix} x_2 \\ x_1 - 1 \end{Bmatrix}; \quad \mathbf{f}_2(\mathbf{X}) = \begin{Bmatrix} x_2 \\ x_1 + 1 \end{Bmatrix} \quad (7a,b)$$

and

$$\mathbf{g}(\mathbf{X}, \tau) = \begin{bmatrix} 0 \\ -A \cos(\Omega\tau + \Psi) - \frac{1}{2} x_2^2 (1 - e^2) \delta(x_1) + \eta(\tau) \end{bmatrix} \quad (8)$$

in which the energy dissipation due to impact is represented by the Dirac delta function (Yim and Lin 1991a). The associated potential energy, $U(x_1)$, and phase portrait are shown in Figs. 2(a) and 2(b), respectively. There exist three fixed points: two saddles at $(+1, 0)$ and $(-1, 0)$, and a center at $(0, 0)$. A pair of heteroclinic orbits are represented by the solid lines in Fig. 2(b), and dashed lines in the same figure represent sample phase trajectories with different initial conditions.

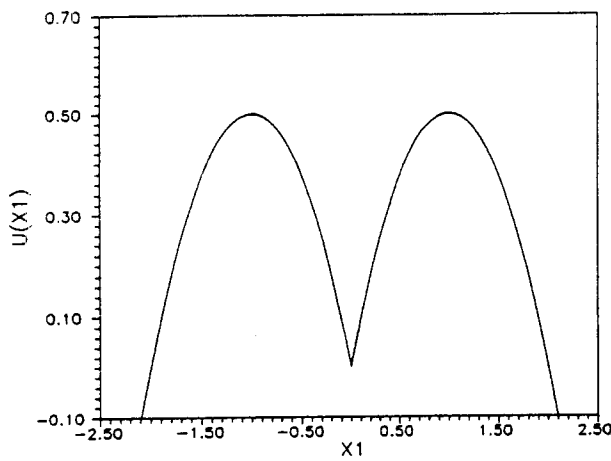
METHODS OF ANALYSIS

A stochastic Melnikov process is derived and the associated average phase-flux rate is computed to demonstrate analytically the relationships between periodic and chaotic, and chaotic and overturning responses. Numerical simulations and mean Poincaré maps are also applied to illustrate the stochastic properties of responses and to identify the existence of embedded attractors.

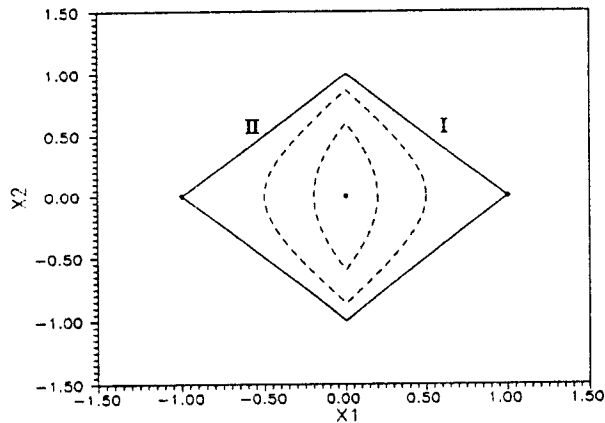
Generalized Stochastic Melnikov Method

The Melnikov method has often been used to obtain a deterministic criterion for chaos in a nonlinear system subjected to periodic excitation (Guckenheimer and Holmes 1983; Wiggins 1988, 1990). This method provides a quantitative representation of the existence of transverse intersections of homoclinic and hyperbolic periodic orbits in a two-dimensional vector field. A generalized version of the Melnikov function for the system subjected to excitation with multiple frequencies was introduced by Wiggins (1990). It was extended to the case of stochastic excitations by Frey and Simiu (1993). Due to its noise-induced random nature, the resulting ensemble of Melnikov functions is called a Melnikov process. A criterion based on the stochastic Melnikov process is developed here to demonstrate noise effects on the existence of chaotic response.

Assuming small perturbations, terms in (6), $x_2^2(1 - e^2)\delta(x_1)/$



(a)



(b)

FIG. 2. (a) Potential and (b) Phase Portrait of Unperturbed (Hamiltonian, $e = 1.0$) Rocking System

2, $A \cos \Omega \tau$, and $\eta(\tau)$, can be scaled by a small parameter ϵ . Then (6) can be rewritten as

$$\dot{\mathbf{X}} = \mathbf{f}_{1,2}(\mathbf{X}) + \epsilon \mathbf{g}(\mathbf{X}, \tau) \quad (9)$$

with $\mathbf{g}(\mathbf{X}, \tau)$ as expressed in (8). The heteroclinic orbits in regions I and II [Fig. 2(b)] can be expressed by explicit time functions (Yim and Lin 1991a)

$$q_i^o(\tau) = (1 - e^{-\tau}, e^{-\tau}) \quad (10)$$

and

$$q_u^o(\tau) = (e^{\tau} - 1, e^{\tau}) \quad (11)$$

respectively. Because of symmetry of the heteroclinic orbits with respect to x_1 in the phase plane, only the upper heteroclinic orbit [(10) and (11)] needs to be examined.

In addition to the periodic excitation and the energy loss due to impact, the external random noise is also considered as another source of perturbation to the heteroclinic orbit. The corresponding stochastic Melnikov process is defined as

$$\begin{aligned} M_r^+(\tau_{10}, \tau_{20}) &= \int_{-\infty}^{\infty} \mathbf{f}[q_{i,u}^o(\tau)] \wedge \mathbf{g}[q_{i,u}^o(\tau); \tau_{10}, \tau_{20}] d\tau \\ &= \int_{-\infty}^0 \mathbf{f}[q_u^o(\tau)] \wedge \mathbf{g}[q_u^o(\tau); \tau_{10}, \tau_{20}] d\tau \\ &+ \int_0^{\infty} \mathbf{f}[q_i^o(\tau)] \wedge \mathbf{g}[q_i^o(\tau); \tau_{10}, \tau_{20}] d\tau \end{aligned}$$

$$= -\frac{2A \cos \Omega \tau_{10}}{1 + \Omega^2} - \frac{1}{2} (1 - e^2) + M_r^+(\tau_{20}) = M_d^+(\tau_{10}) + M_r^+(\tau_{20}) \quad (12)$$

where $M_d^+(\tau_{10})$, due to periodic excitation and impact, represents the mean of the stochastic Melnikov process; $M_r^+(\tau_{20})$, due to random noise, denotes the random portion of the process; and \wedge denotes vector product. Note that for fixed values of τ_{20} , M_r^+ is a Gaussian random variable. A (deterministic) Melnikov criterion provides a necessary condition for chaos (Yim and Lin 1991a), thus the noise effects on the criterion can be demonstrated in an energy (or mean-square) representation. Such a mean-square represented criterion is given by

$$\begin{aligned} \left\langle \left(\frac{1 - e^2}{2} \right)^2 \right\rangle &= \left\langle \left[\frac{2A \cos(\Omega \tau_{10})}{1 + \Omega^2} \right]^2 \right\rangle + \left\langle \left[\frac{-2A \cos(\Omega \tau_{10})}{1 + \Omega^2} \right]^2 \right\rangle \\ &= \langle M_r^+(\tau_{20}) \rangle + \langle M_r^2(\tau_{20}) \rangle = \left[\frac{2A \cos(\Omega \tau_{10})}{1 + \Omega^2} \right]^2 + \sigma_{M_r}^2 \quad (13) \end{aligned}$$

where $\sigma_{M_r}^2$ = variance of the stochastic Melnikov process. The derivation of (13) implicitly incorporates the fact that parameters A , Ω , and e are deterministic and statistically independent of $M_r^+(\tau_{20})$. The stochastic criterion for possible chaotic domain in terms of parameters (A , Ω , e , σ_{M_r}) for chaos in the rocking system is given by

$$\frac{(1 - e^2)^2}{4} \leq \frac{4A^2}{(1 + \Omega^2)^2} + \sigma_{M_r}^2 \quad (14)$$

The variance of $M_r^+(\tau_{20})$, $\sigma_{M_r}^2$, can be obtained by directly integrating the multiple of transfer function $F^2(\Omega)$ and the noise spectrum $S_{\eta}(\Omega)$ over the entire frequency range

$$\begin{aligned} \sigma_{M_r}^2 &= \int_{-\infty}^{\infty} F^2(\Omega) S_{\eta}(\Omega) d\Omega \\ &= \int_{\Omega_{\min}}^{\Omega_{\max}} \frac{4}{(1 + \Omega^2)^2} \frac{\sigma^2}{\Omega_{\max} - \Omega_{\min}} d\Omega = \frac{2\sigma^2}{\Omega_{\max} - \Omega_{\min}} \\ &\cdot \left(\frac{\Omega_{\max}}{\Omega_{\max}^2 + 1} - \frac{\Omega_{\min}}{\Omega_{\min}^2 + 1} + \tan^{-1} \Omega_{\max} - \tan^{-1} \Omega_{\min} \right) \quad (15) \end{aligned}$$

where

$$\begin{aligned} F(\Omega) &= \int_{-\infty}^{+\infty} q_{i,u}^o(\tau) e^{-i\Omega \tau} d\tau = \int_{-\infty}^0 q_u^o(\tau) e^{-i\Omega \tau} d\tau \\ &+ \int_0^{\infty} q_i^o(\tau) e^{-i\Omega \tau} d\tau = \frac{2}{1 + \Omega^2} \quad (16) \end{aligned}$$

Note that the random perturbations considered occupy a continuous frequency range, which may be considered a limiting case of uniformly bounded noises. The continuum of frequencies theoretically may result in unbounded noise amplitudes and hence violate the conditions for insuring the saddle point remaining saddle-type invariant set (Frey and Simiu 1993). Yet, due to its mathematical simplicity, this limiting case is employed here to exhibit asymptotic effects of random noise on the Melnikov function.

The (mean-square represented) upper bound for possible chaotic domain can be obtained by equating the expressions in (14). Criteria for stochastic ($\sigma \neq 0$) and deterministic ($\sigma = 0$) cases in the A - Ω domain are shown by the dashed and solid lines in Fig. 3, respectively. Note that the positive correction term, $\sigma_{M_r}^2$, in (13) lowers the threshold for chaos and enlarges the chaotic domain in the parameter space considered.

Average Phase-Flux Rate

As indicated in the previous section, the chaotic rocking response may occur in the vicinity of the separatrix if the

stable and unstable manifolds intersect. Also the presence of random noise enlarges the possible chaotic domain in the mean-square sense. A close relationship between the chaotic and overturning responses, although intuitively obvious, has not yet been analytically demonstrated in the literature. Non-linear responses under deterministic and stochastic excitations exiting from a chaotic attractor to the overturning regime can be revealed by computing the average flux rate of transport in the phase space (Hsieh et al. 1994; Frey and Simiu 1993). Average rate of phase-space transport across the boundary of "safe" domain can be computed based on the generalized Melnikov process (Hsieh et al. 1994), and noise effects of phase-space transport can then be demonstrated.

The average phase-flux rate is given by

$$\Phi = \lim_{T \rightarrow \infty} \frac{1}{2T} \int_{-T}^T M_g^+(s, \tau_{10}, \tau_{20}) ds$$

$$= E \left\{ \left[\sigma_{M_r} y_1 + \frac{2A}{1 + \Omega^2} y_2 - \frac{1}{2} (1 - e^2) \right]^+ \right\} \quad (17)$$

where Φ = average rate of phase-space transport; and M_g^+ = positive portion of the generalized Melnikov function given by (12). Symbols σ and σ_{M_r} represent the standard deviations of random noise $\eta(\tau)$ and the random portion of stochastic Melnikov process $M_r^+(\tau_{20})$, respectively. Random variables y_1 and y_2 are statistically independent; y_1 = a standard Gaussian variable and $y_2 = \cos U$, where U represents uniformly distributed initial conditions [i.e., $U \sim (0, \pi)$] for the periodic term [(12)] over the upper heteroclinic orbit. The temporal and ensemble averages in (17) are identical due to the fact that periodic excitation is asymptotic mean stationary and the random noise is stationary and ergodic (Frey and Simiu 1993).

The integral in (17) can be carried out by applying the probability distributions of y_1 and y_2 , and integrating over the positive portion of the Melnikov function

$$\Phi = \int_{-1}^1 \int_{\tilde{M}-Dy_2}^{\infty} (\sigma_{M_r} y_1 + Dy_2 - \tilde{M}) p_1(y_1) p_2(y_2) dy_1 dy_2$$

$$= \int_{-1}^1 \left\{ \sigma_{M_r} p_1(\tilde{M} - Dy_2) + (Dy_2 - \tilde{M}) \right.$$

$$\left. \cdot \left[\frac{1}{2} + \frac{1}{\sqrt{2}} \operatorname{erf}(\tilde{M} - Dy_2) \right] \right\} p_2(y_2) dy_2 \quad (18)$$

with

$$\operatorname{erf}(y) = \frac{2}{\sqrt{\pi}} \int_0^y \frac{y^2}{2} dy; \quad p_1(y) = \left(\frac{1}{\sqrt{2\pi}} \right) \exp \left(-\frac{y^2}{2} \right) \quad (19a,b)$$

$$p_2(y) = \frac{1}{\pi \sqrt{1 - y^2}} \quad (19c)$$

where $\operatorname{erf}(\cdot)$ stands for the error function and

$$D = -\frac{2A}{1 + \Omega^2}; \quad \tilde{M} = \frac{1 - e^2}{2} \quad (20a,b)$$

The first term in the integrand of (18), a positive quantity, indicates that the average phase-flux rate is elevated with random noise present. This behavior is also numerically elaborated by the given system parameters in Fig. 4. As discussed in Hsieh et al. (1994), under stochastic excitations, a positive average phase-flux rate strongly indicates occurrences of unbounded response. Hence the presence of random noise increases the possibility of occurrence of overturning as indicated by the positive quantity in (18).

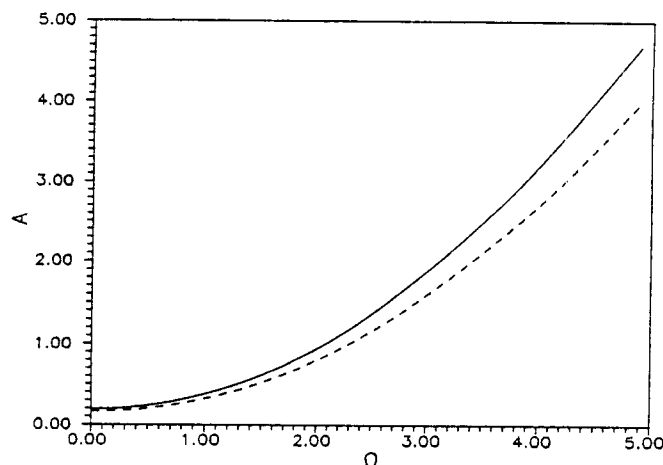


FIG. 3. Melnikov Criteria for Chaotic Rocking Response (Lower Bound in A - Ω Domain): Solid and Dashed Lines Represent Cases without ($\sigma^2 = 0.0$) and with ($\sigma^2 = 0.286$) Noise Disturbance, Respectively [(e, Ψ) = (0.5, 0.0)]

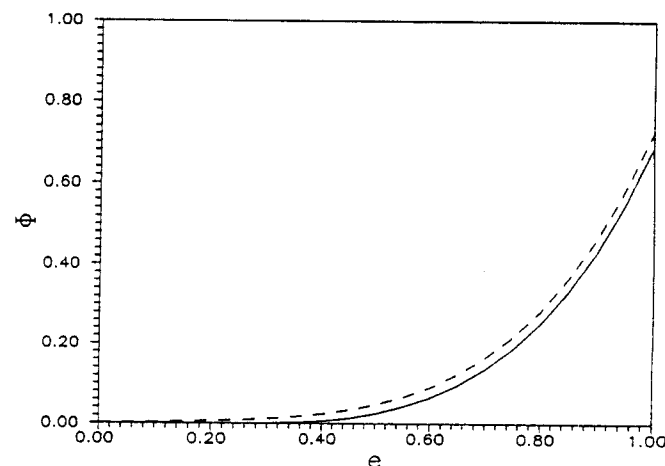


FIG. 4. Average Rate of Phase Flux: Solid and Dashed Lines Represent Cases without ($\sigma^2 = 0.0$) and with ($\sigma^2 = 0.16$) Noise Disturbance, Respectively [(A, Ω, Ψ) = (4.0, 4.0, 0.0)]

Numerical Simulations

Sample paths of the rocking response in a stochastic state can be obtained by directly integrating the stochastic differential equations, (1) and (2), using a fourth-order Runge-Kutta integration algorithm (Yim et al. 1980). The numerical representation of the band-limited noise is introduced in (4). To reach a good approximation of the random noise, the number of harmonics, N , must be relatively large, e.g., $N > 30$ (Kapitaniak 1988). In this study, N is chosen as 100 for an adequate representation.

Mean Poincaré Map

It is well known that the fractal structure of a chaotic attractor can be depicted on the Poincaré map (Thompson and Stewart 1986). However, this structure may be obscured by the presence of random noise. As proposed by Kapitaniak (1988), the noise-induced perturbations can be reduced and the embedded fractal structure can be identified by introducing a mean Poincaré map defined as

$$M_k = \{(E[x_1(t)], E[x_2(t)]) | t = kT, k = 1, 2, \dots\} \quad (21)$$

where T = forcing period; M_k = mean Poincaré point at the k th cycle of forcing period; x_1 and x_2 = displacement and velocity obtained from (6); and $E[x_1]$ and $E[x_2]$ = ensemble averages of x_1 and x_2 , respectively.

The mean Poincaré map takes the ensemble average after each mapping (with interval of the forcing period) to average out the noise effect to reflect the structure of embedded chaotic attractors. In this study, a mean Poincaré point is obtained by averaging 1,200 realizations (numerical simulations) at every forcing period. Here, a mean Poincaré map constitutes 500 mean Poincaré points, i.e., mapping forward in time for 500 cycles of the forcing period. Note that for typical chaotic rocking response, trajectories fall into the steady-state chaotic mode about 5 cycles of the forcing period, and it is sufficient to use 500 points for the purpose of reconstructing embedded attractor.

NOISE-INDUCED TRANSITIONS

The behavior of the rocking system is rich in terms of diverse nonlinear responses (Hogan 1989; Yim and Lin 1991a,b 1992). Among them, the chaotic (long-term unpredictable) and the overturning (unbounded) responses are of most interest. By taking into account the presence of random noise, relationships between these two critical rocking responses are examined in this section.

Noisy Chaotic Response

The noise effects, which have been indicated via Melnikov approach and average phase flux on the chaotic and overturning responses, are twofold. On the one hand, the criterion based on the stochastic Melnikov process provides a necessary condition for chaotic rocking response with the presence of random noise (Fig. 3). The threshold for chaos is lowered by the external random noise and chaotic response may occur in the expanded region. Thus the presence of random noise expedites the occurrence of chaotic response. On the other hand, the chaotic rocking response is closely related to overturning because of the contiguous proximity of their domains of attraction (separated by pseudo-separatrix). The noise-induced elevation in the average flux rate of phase-space transport indicates the region of possible overturning response enlarges with the presence of random noise (Fig. 4). The relationship between chaotic and overturning responses can be demonstrated by using noise intensity as a parameter in the following numerical examples.

The transition from periodic rocking motion to chaotic response is demonstrated in Fig. 5. Fig. 5(a) shows a sample deterministic ($\sigma^2 = 0.0$) periodic response. In the presence of noise the response is chaotic for a finite duration [Fig. 5(b)]. Because of the existence of noise and the weak stability of heteroclinic dynamics, the response trajectory eventually escapes out of the chaotic domain and leads to overturning after 125 cycles of forcing period (transient chaos). Moreover, if the rocking response is chaotic without noise perturbations, it could be brought out of the chaotic state and led to overturning under the presence of random noise.

In summary, these numerical results indicate that the presence of random noise expedites the occurrence of chaotic rocking response, which exists only for a finite duration (thus transient) prior to overturning due to the weak stability of the chaotic attractor.

Note that the velocity restitution coefficient e is chosen 0.5 for chaotic response (Hogan 1989). It is well known that the value of e is closely related to slenderness ratio and materials of block and foundation (Yim et al. 1980), and that 0.5 is low for "slender" blocks. A parametric study on the effects of variations of e over a wide range (from 0.5 to 1.0) is presented in Lin and Yim (1996). Numerical results here identify a close relationship between chaotic rocking response and overturning. They also shed some light on experimental studies on highly nonlinear rocking responses and their stabilities.

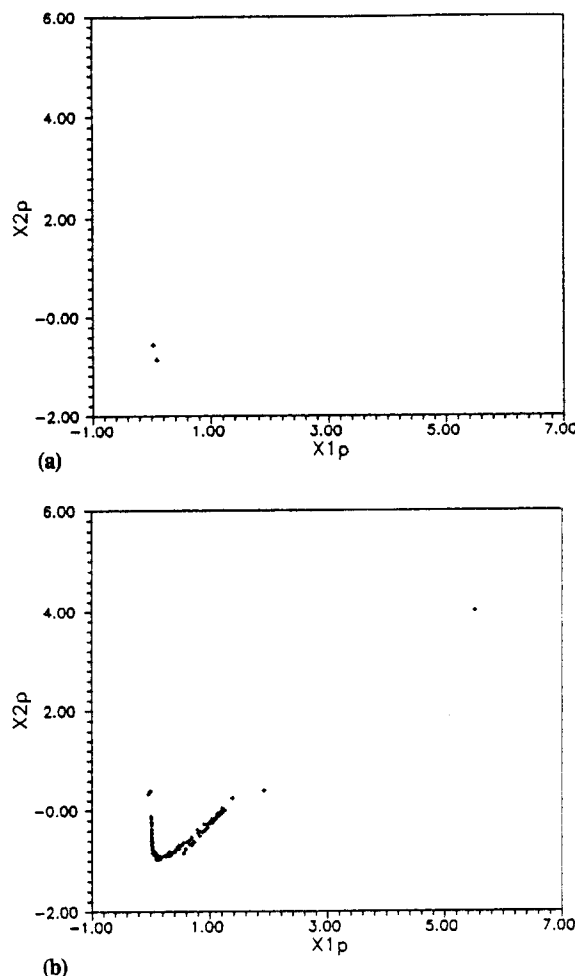


FIG. 5. Noise-Induced Chaotic Rocking Response: (a) Periodic Response with $\sigma^2 = 0.0$; (b) Noise-Induced ($\sigma^2 = 0.05^2$) Transition Chaotic (Strange Attractor in Lower Left Corner) and Overturning (Diverges to Upper Right Corner) Responses, with $(A, \Omega, e, \Psi) = (4.2, 2.7, 0.5, 3.14)$

Noisy Chaotic and Overturning Responses

As shown in the previous section, a close relationship between noisy chaotic and overturning responses has been demonstrated by examining individual realizations. As indicated by Koh (1986), rocking responses are sensitive to excitation details, thus it may be difficult to use time domain simulations to describe the system behavior efficiently and comprehensively. To study the intrinsic behaviors of the rocking response, characteristics that are stable under small random perturbations need to be identified and employed. In this section, the chaos-overturning relationship is examined from a probabilistic point of view via numerical (histogram) approximations of joint probability density functions (JPDFs).

Specifically, large numbers of response realizations are simulated and sampled at multiples of forcing period $2\pi/\Omega$ (Poincaré section), and all of the JPDFs are evaluated numerically by counting the frequency of occurrence (histogram) of the phase trajectories on the discretized Poincaré section. The frequency of occurrence is calculated by counting the number of sampled response realizations falling within each bin and normalizing with respect to the total number of realizations. [To avoid corruption of the histogram, individual samples are assigned a fixed value ($\pi/2$) after overturning.] Thus using the resulting histograms, the joint probability of occurrence (or JPDF) of chaotic or overturning responses can be approximately represented. In this study, 1,000 sample realizations are used to evaluate each JPDF. As indicated in the previous sec-

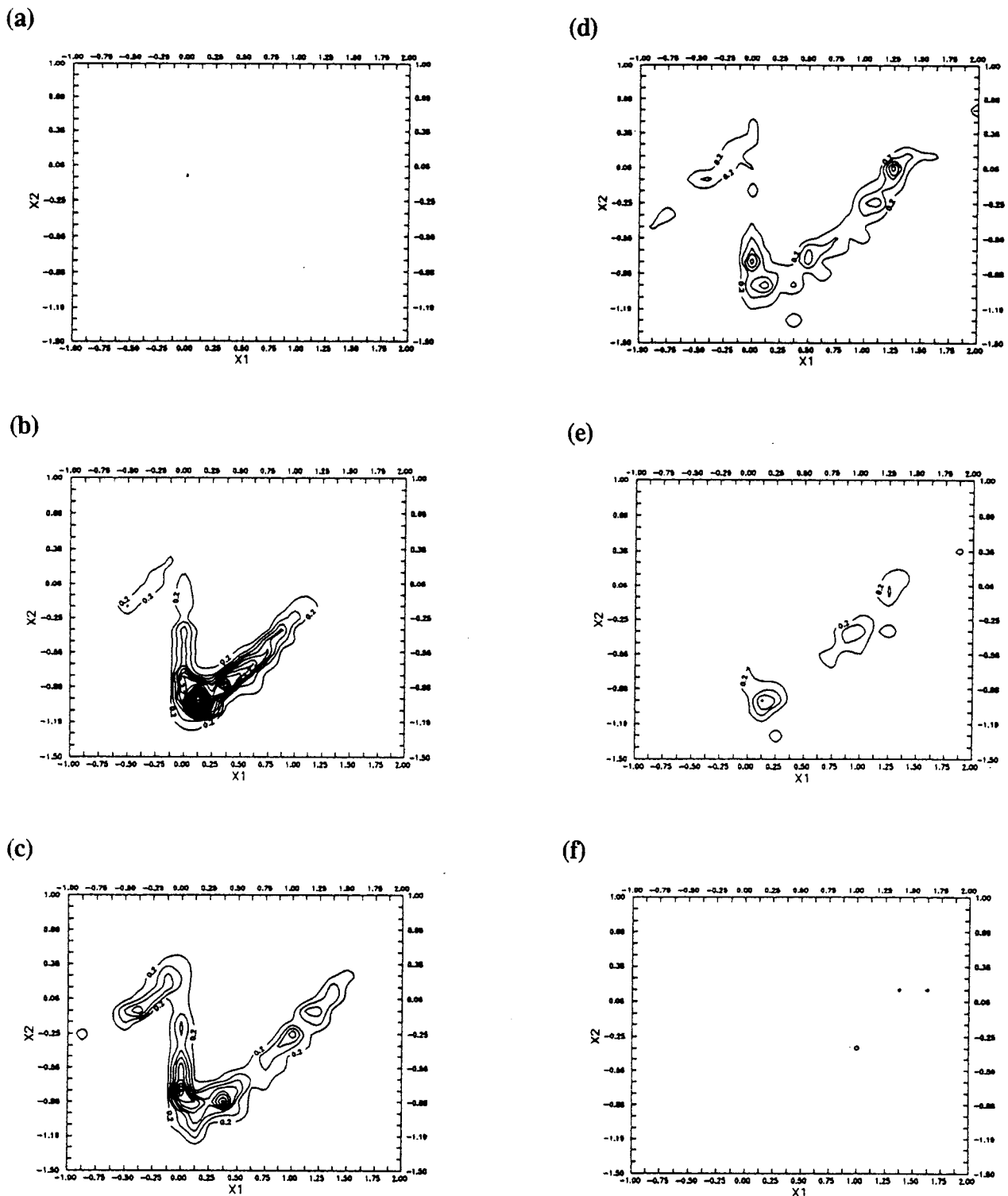


FIG. 6. Evolution of JPDF: (a) Initial Conditions at (0, 0); (b) after 2 Cycles; (c) after 4 Cycles; (d) after 10 Cycles; (e) after 20 Cycles; (f) after 40 Cycles of Forcing Period with $(A, \Omega, e, \Psi) = (4.6, 2.7, 0.5, 3.14)$

tion, chaotic attractors are of weak stability such that the noise energy level is kept low with respect to its deterministic counterpart to illustrate the transition from chaotic to overturning response.

Fig. 6 shows the evolution of the JPDF in the first 40 cycles of excitation period. The noise variance is chosen 0.04, which is relatively small compared to the deterministic component (noise energy/signal energy $\approx 1\%$). Fig. 6(a) shows the JPDF of the deterministic initial conditions, which is essentially a dot in the Poincaré section. The JPDF starts to diffuse and spread over the domain of the chaotic attractor after the first

cycle of the excitation period [Fig. 6(b)]. After 4 cycles, the JPDF can be seen to clearly portray the imprint of a chaotic attractor [Fig. 6(c)]. It is observed that probability (mass) leaks out of the region containing the domain of the chaotic attractor onto the overturning region after 10 cycles [Fig. 6(d)], reflecting the possibility of overturning of the rigid object. Leakage of the probability (mass) to the overturning region becomes more obvious as time elapses [Figs. 6(e) and 6(f)], indicating increasing probability of overturning. Numerical results show that after 60 cycles of the excitation period, the probability of the response trajectories remaining within the chaotic region

becomes negligible, thus, the rocking object overturns with practical certainty.

Evolution of the leakage as demonstrated indicates that the domains of attraction of coexisting chaotic and overturning attractors are bridged by the presence of random noise. Spreading of the JPDP to large values of rocking rotation implies that overturning (diverging to $\pm\pi/2$ rotational displacements) are much stronger attractors compared to other coexisting bounded chaotic attractors. Thus, chaotic response trajectories near the heteroclinic orbit will eventually converge to the overturning region due to the presence of small random noise.

Leakage of the survival probability [Figs. 6(a)–(f)] depends on the noise variance as well as the initial conditions (specified either deterministically or by a distribution) (Soong and Grigoriu 1992). Related properties, such as first passage time, are examined in detail in Lin and Yim (1996). Here, the probability distribution of a specific case of nonoverturning chaotic response within a finite duration is demonstrated by varying noise intensity (i.e., variance, see Fig. 7). Due to the weak stability of the chaotic attractor, the elapsed time is chosen to be 200 cycles of excitation period, and 1,000 sample realizations are used to compute the survival probability. The response realizations are generated with quiescent initial conditions and sampled after 200 cycles of excitation period. Probabilities of nonoverturning chaotic response are obtained by counting the number of trajectories staying within the chaotic domains right after 200 cycles and normalized with respect to the total number of realizations.

Survival probabilities with noise variance varying within the range [0.0 0.04] are shown in Fig. 7. Observe that with no noise present, the chaotic response will not lead to overturning (PDF essentially 1). The probability of nonoverturning (chaotic) response decreases as the noise variance increases. When the noise variance reaches 0.04, the noisy chaotic response will overturn within 200 cycles of excitation period with practical certainty.

Reconstruction of Chaotic Attractor

As demonstrated in previous sections, all chaotic (bounded) motions are weakly stable. Due to the overwhelming strength of the overturning attractor and the noise-induced bridging effect on domains of attraction of coexisting responses, after a sufficiently long but finite duration, all chaotic motions will eventually escape to the overturning region. In practice, except when under very strict artificial control such as in tabletop experiments, noise disturbance of a rocking system is inevitable. Thus, strange attractors embedded in stochastic state and the associated transient chaotic rocking response may be difficult to detect due to the strong attraction of overturning. However, through the mean Poincaré map, the fractal structure of the corresponding embedded chaotic attractor can be reconstructed.

Fig. 8(a) shows a chaotic time history which leads to overturning under the presence of noise disturbance [i.e., transient chaos, also see Fig. 5(b)]. Fig. 8(b) illustrates that when the effects of noise disturbance are averaged out through the mean Poincaré mapping technique, the embedded chaotic attractor can be reconstructed on the Poincaré section. Fractal details in the reconstructed strange attractor imply the existence of hidden "order" in the chaotic response even with noise presence (Kapitaniak 1988), thus transient chaotic rocking responses may be exhibited prior to overturning [Figs. 8(a) and 5(b)].

The capability of the mean Poincaré map to reconstruct chaotic attractors via various noise intensities is further demonstrated in Fig. 9. Compared to the chaotic attractor with no noise perturbations [Fig. 9(a)], the mean Poincaré map preserves the fractal characteristics with a low level noise distur-

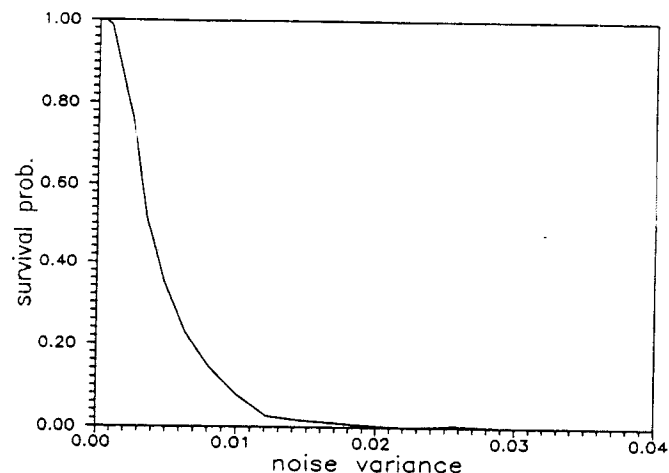
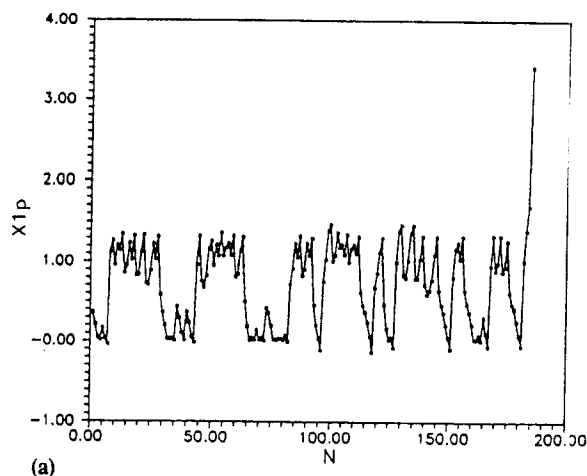
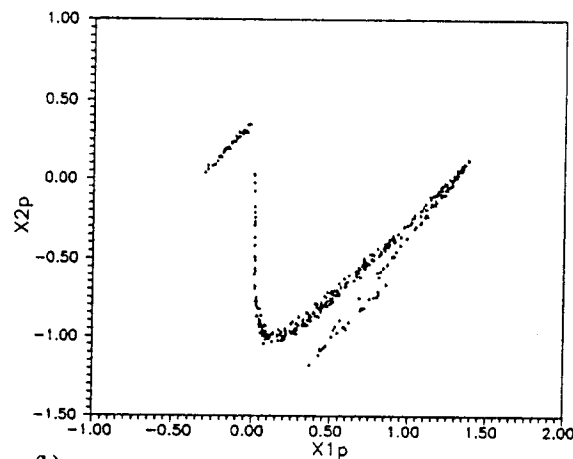


FIG. 7. Survival Probability of Rocking Object for 200 Cycles of Forcing Period with Various Variance ($\sigma^2 \sim [0.0 \ 0.04]$) [(A, Ω, e, Ψ) = (4.6, 2.7, 0.5, 0.0)]



(a)



(b)

FIG. 8. Mean Poincaré Map: (a) Realization of Overturning Rocking Response (Poincaré Point versus N th Cycle of Forcing Period); (b) Corresponding Mean Poincaré Map with 1,200 Realizations [($A, \Omega, e, \sigma^2, \Psi$) = (4.6, 2.7, 0.5, 0.04², 3.14)]

bance [$\sigma^2 = 0.05^2$, Fig. 9(b)]. As the noise variance increases ($0.06^2 \leq \sigma^2 \leq 0.12^2$), even though the mean Poincaré points are still in the bounded region [Figs. 9(c) and 9(d)], the fractal structure of the embedded chaotic attractor deteriorates. This indicates that the "order" of the chaotic response in the stochastic state diminishes as noise intensity increases. Further increases in the noise intensity ($\sigma^2 \geq 0.13^2$) result in overturning response in the mean sense [Figs. 9(e) and 9(f)]. Note that the overturning response in the mean Poincaré is caused

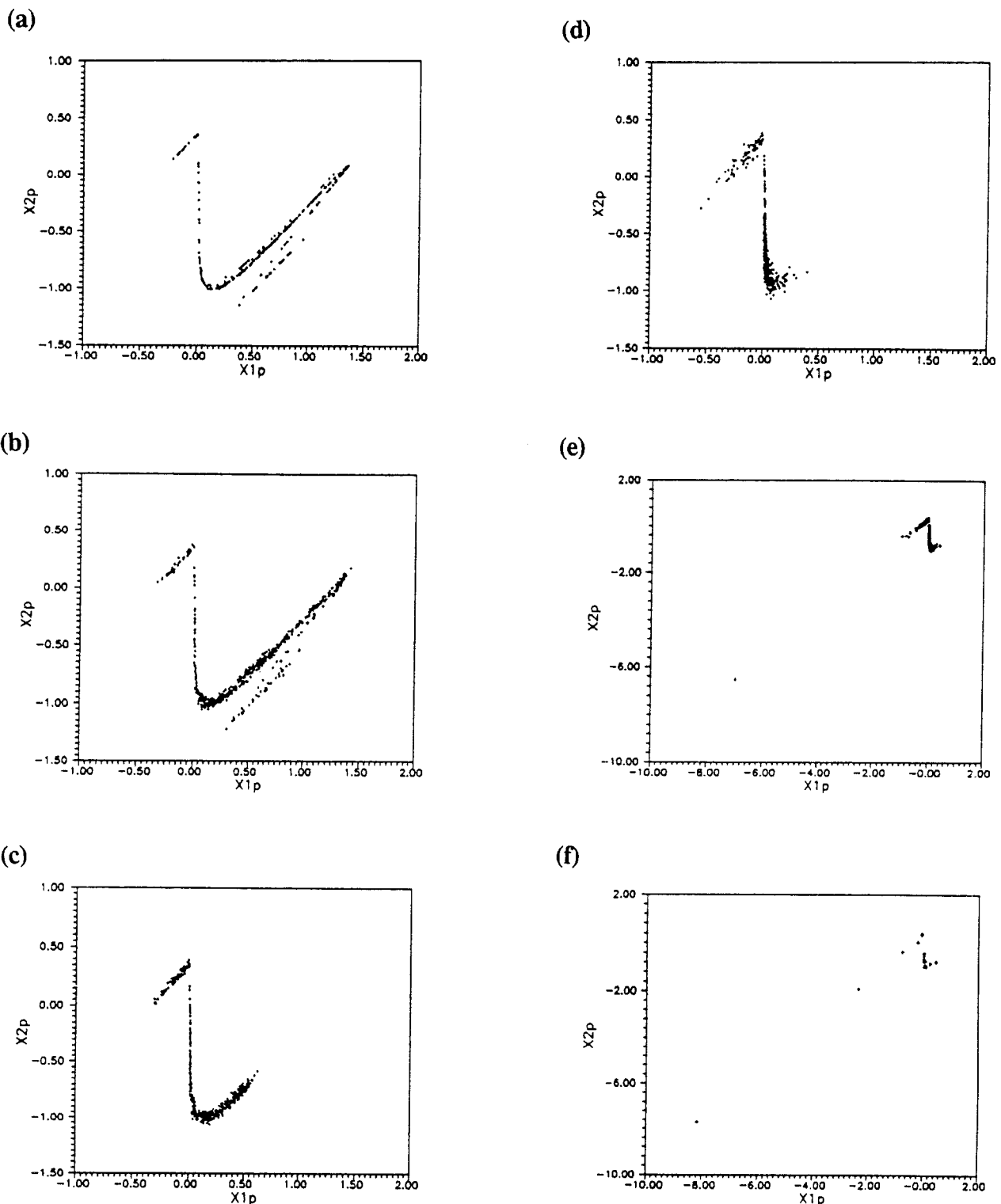


FIG. 9. Capability of Mean Poincaré Map: Mean Poincaré Maps with (a) $\sigma^2 = 0.0$; (b) $\sigma^2 = 0.05^2$; (c) $\sigma^2 = 0.06^2$; (d) $\sigma^2 = 0.12^2$; (e) $\sigma^2 = 0.13^2$; (f) $\sigma^2 = 0.16^2$ [(A, Ω , θ , Ψ) = (4.6, 2.7, 0.5, 3.14)]

by the fact that when divergent (overturning) rocking responses occur, the ensemble average is shifted out of the safe domain, leading to overturning.

CONCLUDING REMARKS

Rocking behaviors of slender rigid objects subjected to periodic excitations with and without noise disturbance have been examined to gain a better understanding of their response stability and sensitivity. Relationships between chaotic and overturning responses in the vicinity of the heteroclinic orbits

have been demonstrated in both deterministic and stochastic states with small random perturbations resulting in the following summary remarks:

1. Taking into account the presence of noise, a mean-square criterion for the possible chaotic domain based on a stochastic Melnikov process has been derived. It is found that the presence of noise enlarges the chaotic domain and expedites the occurrence of chaotic response in the parameter space.
2. Relationships between chaotic and overturning responses

have been analytically examined and demonstrated via the average phase-flux rate based on a stochastic Melnikov process approach. The presence of noise elevates the phase-flux rate and increases the likelihood of overturning. Numerical results also indicate that even with the presence of very weak noise the chaotic response trajectory will eventually be driven to overturning, thus weak stability of deterministic chaotic rocking response is indicated.

3. Numerical results confirm that the presence of noise can induce a transition among diverse rocking responses, e.g., from periodic to "noisy and chaotic," then to overturning. Thus, "noisy and chaotic" response is a possible intermediate state between bounded (periodic) response and overturning.
4. Reconstruction of embedded chaotic attractors in a noisy environment can be accomplished by applying the mean Poincaré map. This mapping technique is able to average out the finite noise effects and to reflect the embedded fractal structure of the attractors. Thus, under the presence of random noise, if the fractal details of reconstructed strange attractors are preserved in the mean Poincaré map, rigid objects will likely experience transient chaotic rocking responses prior to overturning.

ACKNOWLEDGMENT

The writers gratefully acknowledge the financial support from the United States Office of Naval Research (grant No. N00014-92-J-1221).

APPENDIX I. REFERENCES

- Aslam, M., Godden, W. G., and Scalise, D. T. (1980). "Earthquake rocking response of rigid bodies." *J. Struct. Engrg. Div.*, ASCE, 106(2), 377-392.
- Dimentberg, M. F., Lin, Y. K., and Zhang, R. (1993). "Toppling of computer-type equipment under base excitation." *J. Engrg. Mech. Div.*, ASCE, 119(1), 145-160.
- Frey, M., and Simiu, E. (1993). "Noise-induced chaos and phase space flux." *Physica D*, 63, 321-340.
- Guckenheimer, J., and Holmes, P. (1983). *Nonlinear oscillations, dynamical systems, and bifurcations of vector fields*. Springer-Verlag, New York, N.Y.
- Hogan, S. J. (1989). "On the dynamics of rigid-block motion under harmonic forcing." *Proc., Royal Soc. London A*, London, England, 425, 441-476.
- Hsieh, S.-R., Troesch, A. W., and Shaw, S. W. (1994). "Nonlinear probabilistic method for predicting vessel capsizing in random beam seas." *Proc. Royal Soc. London A*, London, England, 446, 195-211.
- Iyengar, R. N., and Manohar, C. S. (1991). "Rocking response of rectangular rigid blocks under random noise base excitations." *Int. J. Nonlinear Mech.*, 26, 885-892.
- Kapitaniak, T. (1988). *Chaos in systems with noise*. World Scientific, Singapore.
- Koh, A. S. (1986). "Rocking of rigid blocks on randomly shaking foundations." *Nuclear Engrg. and Des.*, 97, 269-276.
- Lin, H., and Yim, S. C. S. (1996). "Nonlinear rocking motions. II: overturning under random excitations." *J. Engrg. Mech.*, ASCE, 122(8), 728-735.

- Shinozuka, M. (1971). "Simulation of multivariate and multidimensional random processes." *J. Acoustical Soc. of Am.*, 49, 357-367.
- Soong, T. T., and Grigoriu, M. (1992). *Random vibration of mechanical and structural systems*. Prentice-Hall, Englewood Cliffs, N.J.
- Spanos, P. D., and Koh, A. S. (1984). "Rocking of rigid blocks due to harmonic shaking." *J. Engrg. Mech. Div.*, ASCE, 110(11), 1627-1642.
- Stratonovich, R. L. (1967). *Topics in the theory of random noise. I*. Gordon and Breach, New York, N.Y.
- Thompson, J. M. T., and Stewart, H. B. (1986). *Nonlinear dynamics and chaos*. John Wiley & Sons, Chichester, England.
- Tso, W. K., and Wong, C. M. (1989). "Steady state rocking response of rigid blocks. Part I: analysis." *Earthquake Engrg. and Struct. Dyn.*, 18, 89-106.
- Wiggins, S. (1988). *Global bifurcations and chaos: analytical methods*. Springer-Verlag, New York, N.Y.
- Wiggins, S. (1990). *Introduction to applied nonlinear dynamical systems and chaos*. Springer-Verlag, New York, N.Y.
- Wong, C. M., and Tso, W. K. (1989). "Steady state rocking response of rigid blocks. Part II: experiment." *Earthquake Engrg. and Struct. Dyn.*, 18, 107-120.
- Yim, S. C. S., Chopra, A. K., and Penzien, J. (1980). "Rocking response of rigid blocks to earthquakes." *Earthquake Engrg. and Struct. Dyn.*, 8, 565-587.
- Yim, S. C. S., and Lin, H. (1991a). "Nonlinear impact and chaotic response of slender rocking objects." *J. Engrg. Mech. Div.*, ASCE, 117, 2079-2100.
- Yim, S. C. S., and Lin, H. (1991b). "Chaotic behavior and stability of free-standing offshore equipment." *Oc. Engrg.*, 18, 225-250.
- Yim, S. C. S., and Lin, H. (1992). "Probabilistic analysis of a chaotic dynamical system." *Applied chaos*, J. H. Kim and J. Stringer, eds., John Wiley & Sons, New York, N.Y., 219-241.

APPENDIX II. NOTATION

The following symbols are used in this paper:

- A = $\alpha a/g$, nondimensionalized amplitude of periodic excitation;
 a = amplitude of periodic excitation;
 e = velocity restitution coefficient;
 g = gravitational acceleration;
 I_0 = mass moment of inertia;
 M = object mass;
 M_s = stochastic Melnikov process;
 R = radius of rotation;
 t = time;
 \mathbf{X} = state (displacement and velocity) vector;
 x_1 = state variable (displacement);
 x_2 = state variable (velocity);
 $\alpha^2 = MgR/I_0$;
 η = Shinozuka noise;
 $\Theta = \theta/\theta_{cr}$, nondimensionalized angular displacement;
 θ = angular displacement;
 θ_{cr} = critical angle;
 σ^2 = noise variance;
 $\sigma_{M_s}^2$ = variance of stochastic Melnikov process;
 $\tau = \alpha t$, nondimensionalized time;
 Φ = average phase-flux rate;
 Ψ = phase shift of periodic excitation;
 $\Omega = \omega/\alpha$, nondimensionalized frequency of periodic excitation;
 ω = frequency of periodic excitation.